Eksakta : Berkala Ilmiah Bidang MIPA
VOLUME 27 NO 03 2026, pp 263-274
ISSN : Print 1411-3724 — Online 2549-7464
DOI : https://doi.org/10.24036/eksakta/vol27-iss03/678

Eksakta
Berkala Ilmiah Bidang MIPA
http://www.eksakta.ppj.unp.ac.id/index.php/eksakta

Article

Spatial-Temporal Analysis of b-value Before and After the 2018 Lombok Earthquake Using OK1993 Based on Voronoi in the Bali-NTB Region

Tata Dwi Hardi Yanti[1], Yudha Styawan[1*], Rizki Wulandari[1]

[1]Department of Geophysical Engineering, Faculty of Industrial Technology, Institut Teknologi Sumatera, Lampung, Indonesia.

Article Info

Article history :
Received April 22, 2026
Revised May 20, 2026
Accepted May 26, 2026
Published June 30, 2026
In Press

Keywords :
b-value, OK1993, Voronoi Tessellation, Earthquake, Spatial-Temporal Analysis

Abstract. This study is motivated by the tectonic complexity of the Bali-NTB region, which results in a heterogeneous seismic distribution and active stress dynamics. The objective is to analyze the spatiotemporal evolution of the b-value using the Ogata-Katsura maximum likelihood estimation (OK1993), combined with Voronoi tessellation as an adaptive spatial partition and the Bayesian Information Criterion (BIC) for ensemble model optimization. Spatial analysis prior to the 2018 event revealed a contradiction in the form of high b-value (>1.0) in Lombok. However, the spatiotemporal analysis successfully explains the condition by identifying a zone of low b-value (<1.0) that developed following the 2007 intermediate sized earthquake through the 2018 mainshock distinct from the 2004 local anomaly that did not progress into a major earthquake. This indicates that the persistence of low b-values is a key indicator of high stress accumulation. Following the 2018 earthquake, the high stress zone expanded across Lombok and West Nusa Tenggara (NTB). This study emphasizes the importance of evaluating statistical reliability, such as N(b) and Median Absolute Deviation (MAD), to avoid misinterpreta tions due to data limitations, thereby providing a more reliable frame work for regional seismic hazard assessment.

Corresponding Author :
Yudha Styawan
Departement of Geophysical Engineering, Faculty of Industrial Technology,
Institut Teknologi Sumatera, Lampung, Indonesia.
Email : yudha.styawan@tg.itera.ac.id

1. Introduction

The Bali–West Nusa Tenggara (NTB) region is located within the transitional segment of the Sunda-Banda arc, which was formed by the subduction of the Indo-Australian Plate beneath the Eurasian Plate at a convergence rate of approximately 6–7 cm/year [1]. This tectonic system makes the Bali-NTB region one of the zones with the highest seismic activity in Indonesia and Southeast Asia [1-3]. In addition to being influenced by the megathrust subduction zone south of Bali and NTB, regional deformation is also controlled by the Flores Back-Arc Thrust (FBT), strike-slip faults, and normal faults developing in the waters off Bali, Lombok, and Sumbawa [4–6]. The interaction between these structures results in a heterogeneous distribution of stress accumulation and release, making the seismic pattern in this region complex both spatially and temporally [5-7]. These conditions lead to frequent shallow to intermediate-depth earthquakes in the Bali–NTB region [3],[8].

The regional tectonic complexity is clearly evident in the 2018 Lombok earthquake sequence, which ranks among the most destructive seismic disasters in Indonesia over the past decade [9]. This sequence began with a Mw 6.4 foreshock on July 29, 2018, followed by a Mw 7.0 mainshock on August 5, 2018, a Mw 6.2 earthquake on August 9, 2018, and a Mw 6.9 earthquake on August 19, 2018 [9-10]. Seismological studies indicate that these events occurred on different segments of the FBT system and showed rupture propagation in both westward and eastward directions, suggesting fault segmentation and heterogeneity in the subsurface structure [10-12]. In addition to triggering high aftershock activity, these earthquakes also caused 564 fatalities, displaced more than 417,000 residents, and damaged hundreds of thousands of buildings [13-14]. The magnitude of these impacts underscores the importance of a better understanding of the evolution of tectonic stress and seismic hazard characteristics in the Bali–NTB region.

One of the most commonly used statistical approaches for evaluating seismic characteristics is the Gutenberg–Richter relationship, expressed as $logN = a - bM.$, where N is the cumulative number of earthquakes with magnitude $\geq$ M, while the a-value represents the level of seismic productivity and the b-value represents the ratio between small and large earthquakes [15-16]. The b-value has long been used as an indicator of the mechanical state of the Earth's crust and the level of tectonic stress [17-18]. Low b-values are generally associated with high differential stress, fault asperities, and locked segments that have the potential to generate large earthquakes, whereas high b-values are more frequently associated with rock heterogeneity, low stress conditions, and the influence of crustal fluids [19-21]. Spatial variations in b-values are also known to be related to fault coupling, lithological heterogeneity, and fluid conditions in tectonically active regions [16],[20-23]. Therefore, b-value mapping is widely used to identify asperity zones, seismic gaps, volcanic activity, and areas with the potential for major earthquakes [24-27].

Nevertheless, high-resolution b-value estimates still face methodological challenges, particularly in regions with heterogeneous seismic distributions such as Bali-NTB. Conventional approaches based on fixed grids and sliding time windows often result in spatial aggregation bias because areas with high earthquake density are over-smoothed, while regions with sparse data yield less stable estimates [28-31]. Furthermore, the reliability of b-value estimates is significantly influenced by spatial sampling strategies, the completeness of the earthquake catalog, and magnitude uncertainty [30-32].

To mitigate these limitations, adaptive spatial partitioning methods based on Voronoi tessellation have increasingly been applied in modern seismicity analysis [22],[32-33]. This approach divides the space based on the actual distribution of earthquake events, resulting in a more proportional sample distribution and reducing estimation bias caused by seismicity heterogeneity [21],[33]. On the other hand, the issue of incomplete earthquake catalogs at low magnitudes also poses a significant challenge in b-value analysis [34]. The Ogata-Katsura (OK1993) model was developed by integrating a detection probability function into the frequency magnitude distribution, thereby making b-value estimates more stable across catalogs with varying levels of completeness [35]. The combination of the adaptive Voronoi method and the OK1993 model has proven capable of improving spatial resolution and the

consistency of seismic parameter estimates in regions with clustered seismic activity patterns [21],[32],[35-37].

However, the integrated application of adaptive Voronoi tessellation and the OK1993 estimator to evaluate stress evolution before and after the 2018 Lombok Earthquake remains very limited. Previous studies in the Bali-NTB region generally still use conventional grids and short-term temporal observations [28-29]. Therefore, this study applies the OK1993 frequency–magnitude distribution model combined with adaptive Voronoi tessellation and Bayesian Information Criterion (BIC) optimization [34-35]. The analysis was conducted during the pre-earthquake period (1995–July 2018) and the full earthquake sequence period (1995-2025) to identify changes in the b-value distribution and the evolution of tectonic stress in the Bali-NTB region. This approach is expected to produce more stable, high resolution, and relevant b-value maps to support earthquake hazard studies in the eastern Sunda Arc region.

2. Research Method

2.1 Data Collection and Study Area

The earthquake catalog was obtained from the International Seismological Centre (ISC; www.isc.ac.uk, accessed November 29, 2025), covering the geographic domain of 113.313°-121.157°E and 5.835°-11.56°S, which includes parts of East Java, Bali, Lombok, Sumbawa, and western Flores [38]. The ISC was selected due to its long-term instrumental consistency and its integration of phase data from both regional and teleseismic networks, thereby producing a catalog suitable for multi-decade observation.

All magnitude types in the catalog (Mb, Ms, Ml, Mjma, Mlv) were converted to moment magnitude (Mw) using empirical equations compiled by PuSGeN [8] and Scordilis [39], as summarized in Table 1. Magnitude homogenization is a prerequisite for unbiased b-value estimation because different magnitude scales introduce systematic offsets in the frequency magnitude distribution [21]. After conversion, the catalog was filtered to retain events with a focal depth ≤ 50 km and occurrence times between January 1, 1995, and October 31, 2025.

Aftershocks were not excluded from the catalog in this study because the objective was to evaluate the overall evolution of stress distribution, including the response of the regional seismic system to the major 2018 event. Based on these criteria, the catalog was divided into two temporal groups: the pre-Lombok earthquake period (1995-2018) to isolate stress conditions prior to the major event, and the cumulative period (1995-October 2025) covering the entire sequence of earthquakes along with their post-earthquake evolution.

Table 1. Mw Magnitude Conversion Equations

Magnitude	Conversion Equation	Range	Source
Mb	Mw = 1.010×Mb+0.080	3.7-8.2	
Ms	Mw = 0.601×Ms+2.476	2.8-6.1	PuSGeN [8]
	Mw = 0.923×Ms+0.567	6.2-8.7	
Ml, M	Equivalent to Mw	-	
Mlv	Mw = 0.873×Mlv+0.374	>7	BMKG [3]
Mjma	Mw = 0.58×Mjma+2.25		Scordilis [39]
	Mw = 0.97×Mjma+0.04		

2.2 Adaptive Spatial Partitioning Using Voronoi Tesselation

The high spatial heterogeneity in the distribution of seismicity in the Bali-NTB region motivated the use of Voronoi tessellation as an adaptive spatial partitioning scheme. Unlike a uniform grid, Voronoi cells contract in areas with high event density and expand in sparse areas, ensuring that each cell

contains a proportional and statistically meaningful sample of earthquakes. This adaptive nature is essential to avoid aggregation artifacts that affect conventional grid-based approaches [21],[37].

The number of nodes was systematically varied from 2 to 60 across 59 configurations to explore the trade-off between spatial resolution and estimation stability. Node positions were initialized using two independent strategies: (1) a quasi-random Sobol sequence, which produces a more uniform and homogeneous node distribution; and (2) uniform random sampling as a randomization-based comparison. Each strategy was repeated 50 times in independent replications, resulting in a total of 5,900 candidate models per time period ready for evaluation.

2.3 Estimation of b-Value Parameters OK1993 Model

The constructed Voronoi tessellation was then used as the basis for estimating the b-value parameter in each cell using the maximum likelihood approach developed by Ogata and Katsura (OK1993) [35]. The advantage of this model lies in its ability to explicitly account for the magnitude detection function, which reflects catalog incompleteness at low magnitudes. The detection probability for magnitude M is modeled using the cumulative normal distribution function expressed as

$$q(M|\mu,\sigma) = \frac{1}{\sqrt{2\pi\sigma^2}} \int_{-\infty}^{M} e^{-\frac{(x-\mu)^2}{2\sigma^2}} dx$$

where μ represents the magnitude of completeness and σ describes the sharpness of the detection transition. The probability distribution for the observed magnitudes is then formulated as

$$P(M|\beta,\mu,\sigma) = \frac{\beta e^{-\beta(M-\mu)+\frac{\beta^2\sigma^2}{2}} q(M|\mu,\sigma)}{\int_{-\infty}^{\infty} \beta e^{-\beta(M-\mu)+\frac{\beta^2\sigma^2}{2}} q(M|\mu,\sigma) dM}$$

with the scale parameter β linking the b-value to the exponential distribution. The log-likelihood function for n earthquake events in a Voronoi cell is then formulated completely as

$$\ln L(\theta) = n \ln \beta - \Sigma_{i=1}^{n} [\beta M_i - \ln q\ (M_i|\mu,\sigma)] + n\beta\mu - \frac{n\beta^2\sigma^2}{2}$$

where θ is estimated through an optimization process using a trust-region algorithm with constraints that ensure convergence to the global solution [40]. As the initial point of the optimization, the initial b-value is calculated using the classical estimator introduced by Aki [41] with the formula

$$b_{MLE} = \frac{\log_{10}(e)}{\bar{M} - M_{min}}$$

where $\bar{M}$ is the average magnitude and M_{min} is the minimum magnitude in the cell. To ensure that the estimates have an adequate statistical foundation, each Voronoi cell is required to contain at least five earthquake events; cells with data counts below this threshold are not assigned a b-value estimate. Table 2. provides an explanation of the key parameters used in the analysis.

Table 2. The Parameters of the OK1993 Model and Their Physical Significance

Parameter	Symbol	Physical meaning
Scale parameter	β	Parameters of the exponential distribution; $\beta = b \cdot ln(10)$
Magnitude of completeness	μ	Magnitude at a 50% detection probability, catalog completeness threshold
Standard deviation	σ	Detection transition width
Detection function	$q(M\|\mu,\sigma)$	The probability that an earthquake of magnitude M is recorded in the catalog based on the cumulative normal distribution function

2.4 Model Selection, Uncertainty Quantification and Spatiotemporal Cross-Section Analysis

An objective selection procedure based on the Bayesian Information Criterion (BIC) was applied to 5,900 candidate models to identify the optimal ensemble. This study applies the Bayesian Information Criterion (BIC), which is formulated as

$$BIC = -\ln(L) + \frac{k}{2}\ln n$$

where ln L represents the maximum log-likelihood of the model, k is the number of parameters, and n is the total number of observations. In this research, we divided n by 100 to prevent the distribution from skewing heavily toward very low cell counts, ensuring a balance between low and high cell counts. The BIC criterion systematically balances two important components: the first component measures how well the model explains the observed data, while the second component provides a penalty for model complexity to prevent overfitting. Models with lower BIC values indicate a more optimal trade-off between these two aspects.

From all candidate models, the 100 models with the lowest BIC values are selected to form the best ensemble to be used in the subsequent analysis stage. The final b-value at each grid point is then calculated as the median of the distribution of estimates produced by the 100 selected models, providing an estimator that is robust to extreme values. The level of uncertainty is quantified using the Median Absolute Deviation (MAD), which is chosen due to its robustness to outliers compared to conventional standard deviation and its direct representation of dispersion around the median value.

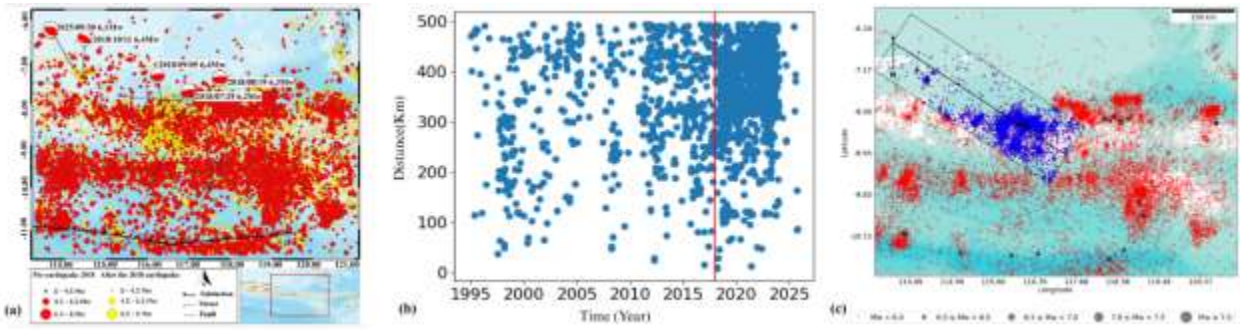

Figure 1. (a) Seismicity map of the Bali-West Nusa Tenggara region for the period 1995-2025. (b) Earthquake distribution along the distance-time profile diagram. (c) Map showing the location of the spatial-temporal cross-section profile A-A' (the selected profile represents the region with a sequence of large earthquakes occurring throughout 1995-2025 with magnitudes above 6).

The spatial analysis is complemented by a study of the spatial-temporal evolution of b-value through a cross-section approach designed to capture temporal dynamics along the main deformation zone. The study area is mapped into an evaluation grid of 200 × 200 points, accompanied by a boundary extension of 0.09° on each side to minimize edge effects that may influence results in the boundary zones of the study area. A linear profile with a length of ±500 km is constructed with an orientation aligned with the sequence of large earthquakes occurring in the region. All earthquakes located within a buffer zone of ±80 km from the profile line are projected orthogonally to obtain distance coordinates along the profile.

The earthquake occurrence time, recorded in year-month-day format, is converted into decimal years simultaneously to facilitate continuous analysis in the temporal domain. Distance and time values are normalized using the z-score transformation defined as $z=(x-\mu)/\sigma$, where μ and σ are the

mean and standard deviation of the variable distribution, respectively, with the aim of integrating spatial and temporal dimensions within a consistent analytical framework.

The previously described methodological approach Voronoi tessellation as an adaptive spatial partitioning method and OK1993 estimation as the parameter calculation method is then reapplied to a two-dimensional space consisting of normalized time and normalized distance. This method enables the identification of b-value variation patterns not only in a geographic spatial context but also in terms of how the parameter evolves along the temporal axis, particularly in identifying changes in seismicity characteristics before and after the 2018 Lombok earthquake within an integrated spatial-temporal framework.

3. Results and Discussion

The spatial distribution of the b-value parameter for the Lombok earthquakes was analyzed through the results of model optimization using the Bayesian Information Criterion (BIC), median b-value, Median Absolute Deviation (MAD), and the number of valid ensemble models N(b). The curve showing the relationship between the number of nodes and the BIC value indicates a significant decrease at lower node counts before reaching a stable minimum value (Figure 2.a). This condition indicates that models with a certain number of nodes are able to represent the complexity of the data distribution without producing overfitting. The model with the minimum BIC value is selected as the optimal configuration for estimating the Voronoi tessellation parameters.

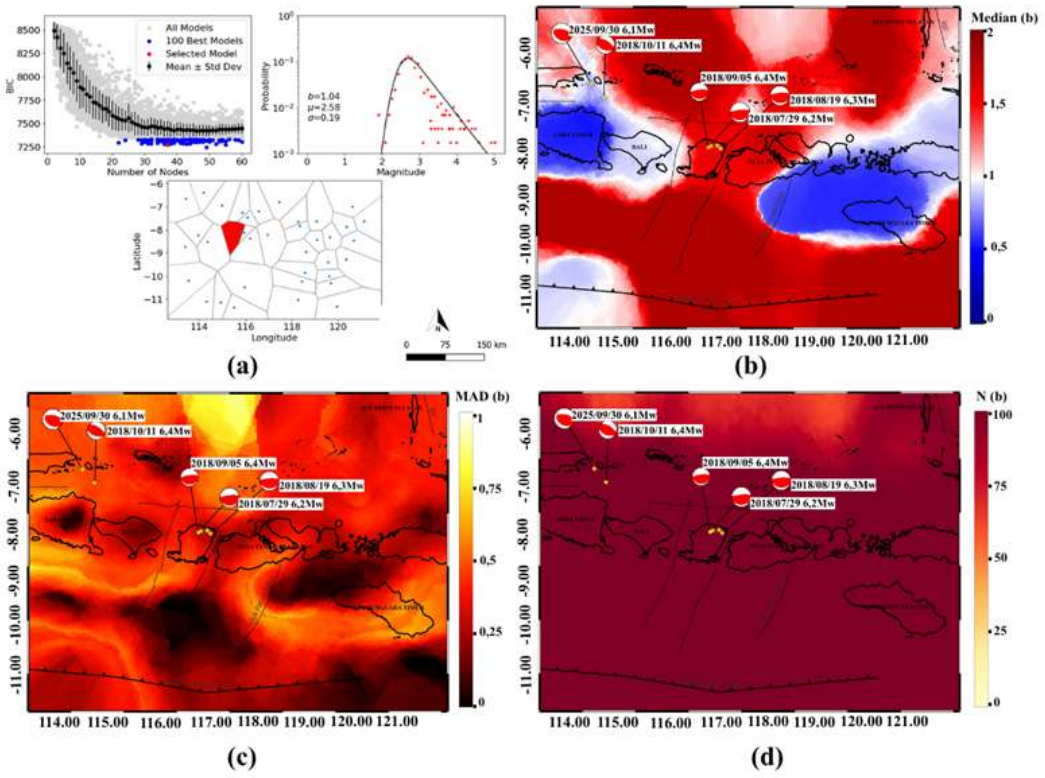

Figure 2. (a) Distribution of BIC with respect to nodes. Inset map shows the Voronoi tessellation from the selected model with the red polygon highlighting the selected sample cell for the probability curve. (b) Median of b-value for the pre-2018 Lombok earthquake period. (c) Median Absolute Deviation (MAD). (d) N(b), total coverage of overall b-value.

Spatial analysis of the pre-earthquake period in Lombok in 2018 (1995-July 2018) shows that the distribution of b-values in the Bali–NTB region exhibits a heterogeneous pattern that reflects variations in regional tectonic stress conditions. The b-values range from approximately 0.5 to over 1.5, with low values (<0.8) dominating in eastern East Java and parts of Bali. Meanwhile, the Lombok region and western NTB exhibit relatively higher b-values (>1.0).

Areas with low b-values are interpreted as regions experiencing higher differential stress accumulation and having the potential to generate large-magnitude earthquakes [16]. Conversely, high b-values indicate a predominance of small earthquakes, greater rock heterogeneity, or relatively lower stress conditions. Thus, the pre-2018 distribution pattern indicates that the region from northern East Java to Bali had experienced significant tectonic stress concentration prior to the 2018 Lombok earthquake sequence.

On the other hand, prior to 2018, the Lombok region was still dominated by medium to high b-values. This condition indicates that stress accumulation at that time was not yet extremely concentrated on a regional spatial scale. However, spatial analysis has not yet been fully capable of describing the temporal evolution of the stress accumulation process leading up to major earthquakes. Therefore, temporal analysis is necessary to understand the dynamics of the seismic system more comprehensively.

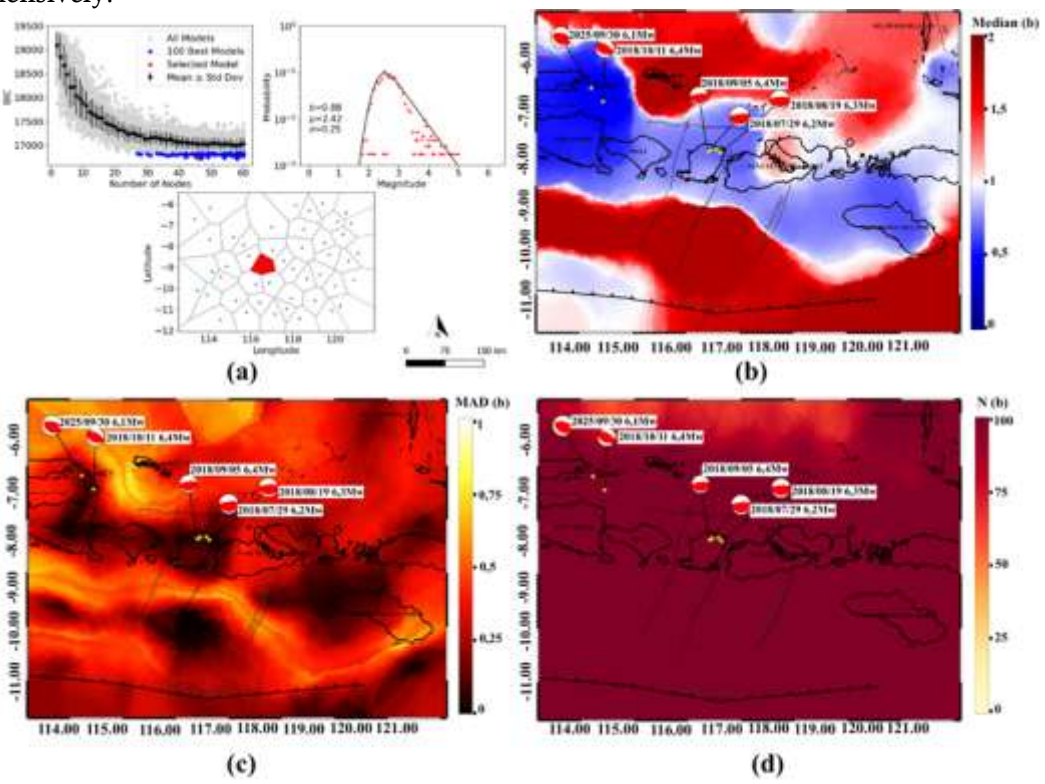

Figure 3. (a) Distribution of BIC with respect to nodes. Inset map shows the Voronoi tessellation from the selected model with the red polygon highlighting the selected sample cell for the probability curve. (b) Median (b-value) for the period up to post-Lombok earthquake (1995-2025). (c) Median Absolute Deviation (MAD). (d) N(b), total coverage of overall b-value

For the cumulative period from 1995 to 2025 (Figure 3), which includes the 2018 Lombok earthquake sequence and post-earthquake activity, the distribution of b-values shows significant spatial changes compared to the pre-earthquake period. Zones with low b-values (<0.8) have expanded more widely and form an elongated pattern oriented northwest–southeast, covering the regions of

Lombok, Bali, western Sumbawa, and parts of East Java. This change in pattern indicates a redistribution and re-concentration of tectonic stress following the 2018 mainshock. The persistence of low b-value zones in the post-earthquake period suggests that the energy release during the mainshock has not fully reduced the accumulated stress in the region. Conversely, the stress transfer process is suspected to have triggered an increase in stress concentration along the surrounding fault segments.

The presence of zones with very low b-values (<0.8) that persisted into the post-earthquake period also indicates the dominance of relatively large-magnitude earthquakes over small ones. This suggests that the tectonic system in the Bali–NTB region remains in an active phase and has not yet undergone comprehensive seismic relaxation. Methodologically, this spatial pattern can be identified more clearly through the application of adaptive Voronoi tessellation, which is capable of maintaining a more proportional distribution of earthquake samples in areas with high levels of seismicity heterogeneity. This approach is effective in reducing the over-aggregation effect commonly found in conventional uniform grid methods.

The distributions of MAD and N(b) for both periods show consistent and complementary patterns. During the pre-earthquake period (1995–2018), MAD was dominated by low values (<0.3) in the Bali and Lombok regions, reflecting the stability of the b-value estimates, although high values (>0.5) still occurred off the northern and southern coasts due to data limitations. The dominant N(b) distribution >90 confirms good and representative ensemble coverage. In the post-earthquake period (1995–2025), MAD remained low with a more even spatial distribution, while N(b) was consistently high across nearly the entire study area, indicating improved reliability of b-value estimates. Overall, the analysis of these two parameters validates that the increase in post-event earthquake data from the 2018 Lombok earthquake significantly contributes to improved quality of b-value estimates across the entire study area.

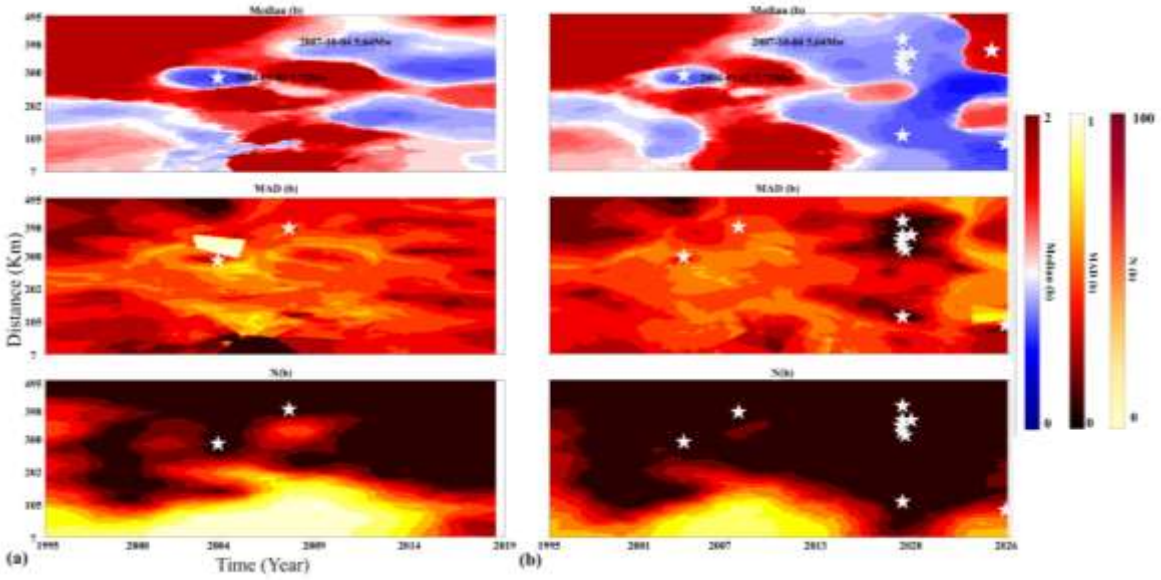

Figure 4. Temporal visualization along profile A-A′: (a) Pre-2018 Lombok earthquake period (1995-July 28, 2018). (b) Cumulative period including the post-2018 Lombok earthquake sequence (1995-2025). White stars indicate the occurrences of significant earthquakes with magnitude Mw ≥ 5.5.

Based on spatial analysis (Figure 2), the region around Lombok Island exhibited relatively high b values (> 1.0) prior to the 2018 earthquake sequence, whereas the region in northern East Java was dominated by lower values approaching 1.0. Theoretically, this spatial distribution indicates a clear contradiction; major earthquakes are typically preceded by a period of significant tectonic stress accumulation, which should be marked by a clear decrease in the b-value (< 1.0) in the future epicenter region[30].

To clarify this difference, a temporal analysis along the spatio-temporal profile (Figure 4) provides a more dynamic picture. The temporal profile shows that the b-value in the Lombok segment did indeed drop to < 1.0 prior to the 2018 mainshock. Interestingly, this precursor "blue zone" (low b-value anomaly) was preceded by a moderate earthquake (5.64 Mw) on October 4, 2007, after which the low b-value zone expanded and persisted. In contrast, another low b-value zone was observed earlier around the January 2, 2004, event (5.72 Mw); however, this anomaly remained localized and did not persist, so no subsequent major earthquake occurred at that location.

This difference highlights a crucial seismological pattern: a consistently low b-value (< 1.0) over a long period is a strong indication of ongoing stress accumulation leading to a major earthquake, whereas a temporary or non-sustained decrease in the b-value indicates local stress variations that do not result in a major fault rupture.

Furthermore, an unexplained anomaly is observed north of East Java, where a persistent low *b*-value zone appeared without being preceded by a moderate earthquake (Mw > 5.5). However, this specific observation must be interpreted with caution. Given the remarkably low N(b) values between 2001-2013, it is difficult to conclusively determine whether this low *b*-value zone represents genuine tectonic stress accumulation or is merely a statistical artifact arising from catalog incompleteness and limited data coverage in the area.

In the period up to post-earthquake (1995-2025), the temporal pattern becomes more structured. Low b-value zones (<0.8) develop more extensively and persistently at distances of approximately 300-450 km after 2018, associated with increased seismic activity following the Lombok earthquake. A decrease in b-value along the profile at approximately 398 km had already begun to be identified around 2007 and was followed by significant earthquake activity in 2018 at a relatively similar location. This condition causes the b-value in this profile to remain low into the post-mainshock period, representing a relatively high concentration of stress and the dominance of larger-magnitude earthquake events over a long time span. The MAD distribution in this period is dominated by low values (<0.3), especially after 2018, indicating improved stability of estimation as the number of earthquake data increases.

These findings offer a critical advancement over recent studies in the region, particularly the work by Hamidah et al. [28]. While studies fundamentally agree that the Lombok and West Nusa Tenggara region is a high-stress zone characterized by low *b*-values, there are significant differences in the temporal evolution captured by the differing methodologies. Hamidah et al. [28] utilized a conventional uniform spatial grid and a sliding time-window approach, reporting a short-term precursory increase in the *b*-value (up to 1.4-1.5) followed by a sudden drop immediately preceding the 2018 mainshock. Furthermore, they observed a relatively constant *b*-value (around 1.0) in the post-earthquake period.

In contrast, the adaptive Voronoi tessellation and OK1993 ensemble modelling employed in this study reveal a markedly different and more nuanced dynamic. Instead of a sudden short-term fluctuation, our spatial-temporal profile demonstrates that a persistent low *b*-value anomaly (<1.0) had already been developing steadily since 2007 at the 300-450 km of the cross-section, serving as a long-term indicator of locked stress. Additionally, rather than remaining constant after the mainshock, our results show a significant expansion and deepening of the extreme low *b*-value zone (<0.8) across the spatial profile. This indicates an ongoing and complex tectonic stress redistribution rather than a static post-seismic relaxation. This striking discrepancy highlights the distinct advantage of using an

adaptive spatial partition combined with maximum likelihood estimation that strictly accounts for catalog incompleteness, thereby mitigating the statistical artifacts often produced by uniform grids and fixed temporal windows.

4. Conclusion

This study demonstrates that relying solely on spatial *b*-value mapping can obscure critical precursory signals of major earthquakes. While spatial analysis prior to the 2018 Lombok earthquake indicated deceptively high *b*-values (>1.0) in the epicentral region, spatial-temporal cross-section analysis successfully captured a persistent low *b*-value anomaly (<1.0) developing after 2007. The comparison between this persistent anomaly and a previous transient one in 2004 emphasizes a crucial seismological behavior: the duration and stability of a low *b*-value zone are key indicators of significant tectonic stress accumulation leading to a large rupture, whereas short-lived drops indicate localized stress variations. Following the 2018 mainshock, this high-stress zone expanded persistently across Lombok and West Nusa Tenggara. Finally, the study highlights the absolute necessity of incorporating statistical reliability parameters, specifically MAD and the ensemble coverage *N(b)*. By evaluating these parameters, statistical artifacts caused by catalog incompleteness such as the unverified anomaly north of East Java can be isolated from the interpretation, thereby providing a more accurate and robust foundation for future earthquake hazard mitigation strategies.

References

[1] Hutchings, S. J., & Mooney, W. D. (2021). The seismicity of Indonesia and tectonic implications. *Geochemistry, Geophysics, Geosystems*, 22(9), e2021GC009812.

[2] Irsyam, M., Cummins, P. R., Asrurifak, M., Faizal, L., Natawidjaja, D. H., Widiyantoro, S., Meilano, I., Triyoso, W., Rudiyanto, A., Hidayati, S., Ridwan, M., Hanifa, N. R., & Syahbana, A. J. (2020). Development of the 2017 national seismic hazard maps of Indonesia. *Earthquake Spectra*, 36(1_suppl), 112–136.

[3] BMKG. (2022). *Katalog Gempabumi Signifikan dan Merusak Indonesia Tahun 1821–2022*. Jakarta, Indonesia.

[4] Felix, R. P., Hubbard, J. A., Bradley, K. E., & Lythgoe, K. H. (2022). Tsunami hazard in Lombok and Bali, Indonesia, due to the Flores back-arc thrust. *Natural Hazards and Earth System Sciences*, 22, 1665–1682

[5] Andikagumi, H., Natawidjaja, D. H., Daryono, M. R., Horspool, N., & Cartereau, B. (2024). The Flores Thrust and its interplay with volcanism. *Tectonics*, 43, e2024TC008269.

[6] Natawidjaja, D. H. (2018). Major active faults in Indonesia: Implications for seismic hazard and tectonic evolution. *Geological Society, London, Special Publications*, 441(1), 7–26.

[7] Hisyam, F., Susilo, A., Anshori, M., & Hasan, M. F. R. (2024). Spatio-temporal variation seismicity pattern in East Java between 2002 and 2022 based on the b-value and seismic quiescence z-value. *Trends in Sciences*, 21(4), 7608.

[8] PUSGEN. (2017). *Peta Sumber dan Bahaya Gempa Indonesia Tahun 2017*. Bandung, Indonesia.

[9] BMKG. (2018). *Laporan Gempabumi Lombok 2018*. Jakarta, Indonesia.

[10] Supendi, P., Nugraha, A. D., Widiyantoro, S., Pesicek, J. D., Thurber, C. H., Abdullah, C. I., Daryono, Wiyono, S. H., Shiddiqi, H. A., & Rosalia, S. (2020). *Relocated aftershocks and background seismicity in eastern Indonesia shed light on the 2018 Lombok and Palu earthquake sequences*. *Geophysical Journal International*, 221(3), 1845–1855.

[11] Afif, H., Nugraha, A. D., Muzli, M., Widiyantoro, S., Zulfakriza, Z., Wei, S., et al. (2021). *Local earthquake tomography of the source region of the 2018 Lombok earthquake sequence, Indonesia*. Geophysical Journal International, 226(3), 1814–1823.

[12] Salman, R., Tay, C. W. J., Hill, E. M., Lindsey, E. O., Costa, F., Lythgoe, K. H., Bradley, K. E., Muzli, Yun, S. H., Wei, S., & Chin, S. T. (2020). *Cascading partial rupture of the Flores thrust*

during the 2018 Lombok earthquake sequence, Indonesia. *Seismological Research Letters*, 91(4), 2155–2165.
[13] BNPB. (2018). *Laporan Penanganan Gempa Lombok 2018*. Jakarta, Indonesia.
[14] Wibowo, S. B., Hadmoko, D. S., Isnaeni, Y., Farda, N. M., Putri, A. F. S., Nurani, I. W., & Supangkat, S. H. (2021). Spatio-temporal distribution of ground deformation due to 2018 Lombok earthquake series. *Remote Sensing*, 13(11), 2222.
[15] Gutenberg, B., & Richter, C. F. (1944). Frequency of earthquakes in California. *Bulletin of the Seismological Society of America*, 34, 185–188.
[16] Convertito, V., Tramelli, A., & Godano, C. (2024). B map evaluation and on-fault stress state for the Antakya 2023 earthquakes. *Scientific Reports*, 14, 1546.
[17] Ito, Y., Kaveh Fathian, A., Okuda, T., & Uchida, N. (2023). Physical mechanism for a temporal decrease of the Gutenberg-Richter b-value prior to a large earthquake. *Journal of Geophysical Research: Solid Earth*, 128, e2023JB027413.
[18] Utsu, T. (1999). Representation and analysis of the earthquake size distribution. *Pure and Applied Geophysics*, 155, 509–535.
[19] Schorlemmer, D., Wiemer, S., & Wyss, M. (2005). Variations in earthquake-size distribution across different stress regimes. *Nature*, 437, 539–542.
[20] Convertito, V., Tramelli, A., & Godano, C. (2024). Evaluation of the b maps on the faults of the major (M > 7) South California earthquakes. *Earth and Space Science*, 11, e2023EA002933.
[21] Kamer, Y., & Hiemer, S. (2013). Data-driven spatial b-value estimation without magnitude scale dependencies. *Bulletin of the Seismological Society of America*, 103(4), 2299–2309.
[22] Ningrum, R. W., Suryanto, W., Kamaruddin, B., Wahyudi, Sholihun, Wibowo, N. B., Arif, A. K. D., Aswan, M., Raharjo, W., Hesti, & Saprudin. (2024). Characteristics of earthquake hazards in jailolo, west halmahera, indonesia: An analysis of *b* values and site dynamics. *International Journal of Geophysics*, *2024*(1), 5594818.
[23] Hu, X., Chen, Y., Lin, T.-W., Hsu, S.-K., Kuo, K.-W., Shin, T.-C., & Leu, P.-L. (2024). Spatial-temporal variations of b-values prior to medium-to-large earthquakes in Taiwan and the feasibility of real-time precursor monitoring. *Earth, Planets and Space*, 76, 122.
[24] Prasetio, A. D., Anggono, T., Syuhada, S., Hasib, M., Febriani, F., Sulaiman, A., & Dewi, C. N. (2022). *Spatial variation of b-values correlation with tectonic activity along the Southern Java subduction zone*. AIP Conference Proceedings, 2652, 030005.
[25] Nanjo, K. Z., Izutsu, J., Orihara, Y., & Kamogawa, M. (2022). Changes in seismicity pattern due to the 2016 Kumamoto earthquake sequence and implications for improving the foreshock traffic-light system. *Tectonophysics*, 822, 229175.
[26] Gulia, L., Wiemer, S., Biondini, E., Enescu, B., & Vannucci, G. (2024). Improving the foreshock traffic light systems for real-time discrimination between foreshocks and aftershocks. *Seismological Research Letters*, 95(6), 3579–3592.
[27] Chen, H., Wang, Y., Zhang, Y., & Jiang, C. (2025). b-Value evaluation and applications to seismic hazard assessment. *Entropy*, 27(9), 958.
[28] Hamidah, N., et al. (2020). Spatial and temporal b-value analysis of Lombok earthquakes. *Indonesian Journal of Geophysics*, 21, 45–56.
[29] Rohadi, A., et al. (2021). Temporal seismicity changes before the Lombok earthquake. *Journal of Seismology*, 25, 337–352.
[30] Gong, W., Chen, H., Gao, Y., Jiang, C., & Liu, J. (2024). A test on methods for Mc estimation and spatial-temporal distribution of b-value in the eastern Tibetan Plateau. *Frontiers in Earth Science*, 12, 1335938.

[31] Wang, J., et al. (2025). Estimating magnitude completeness in earthquake catalogs: A comparative study of catalog-based methods. *Journal of Geophysical Research: Solid Earth*, 130, e2025JB031441.
[32] Iwata, T., & Nanjo, K. Z. (2024). Adaptive estimation of the Gutenberg-Richter b value using a state space model and particle filtering. *Scientific Reports*, 14, 5665.
[33] Mao, S., Ellsworth, W. L., & Beroza, G. C. (2023). Adaptive coda-wave imaging with Voronoi tessellation. *Journal of Geophysical Research: Solid Earth*, 128, e2023JB026592.
[34] Taroni, M. (2023). Estimating the magnitude of completeness of earthquake catalogs using a simple random variable transformation. *The Seismic Record*, 3(3), 194–199.
[35] Ogata, Y., & Katsura, K. (1993). Analysis of temporal and spatial heterogeneity of magnitude-frequency distribution. *Geophysical Journal International*, 113, 727–738.
[36] Mizrahi, L., Nandan, S., & Wiemer, S. (2021). The effect of declustering on the size distribution of mainshocks. *Seismological Research Letters*, 92, 2333–2342.
[37] Yin, F., & Jiang, C. (2024). Enhanced b-value time-series calculation method using data-driven approach. *Geophysical Journal International*, 236(1), 78–87.
[38] Styawan, Y. (2025). Quakesee: Aplikasi cross-platform python berbasis web untuk otomasi dan aksesibilitas dalam pengunduhan data gempa terbuka. *Jurnal Pendidikan, Sains, Geologi, dan Geofisika (GeoScienceEd Journal)*, 6(3), 1292–1301.
[39] Scordilis, E. M. (2006). Empirical global relations converting MS and mb to moment magnitude. *Journal of Seismology*, 10(2), 225–236.
[40] Styawan, Y. (2025). Optimizing seismic b-values in the Java region through Voronoi-based OK1993 modelling. *JGE (Jurnal Geofisika Eksplorasi)*, 11, 109–121.
[41] Aki, K. (1965). Maximum likelihood estimate of b in the formula log N=a-bM and its confidence limits. *Bulletin of the Earthquake Research Institute*, 43, 237–239.